Phenomenological Introduction to Neutrino Oscillations

Tanjona R. Rabemananjara*
Universita degli Studi di Milano
Via Celoria 16, Milano 20133, Italy

I. INTRODUCTION

Since the idea of neutrino oscillations has been hypothesized by Potencorvo in 1957 [1, 2], important experimental and theoretical developments have emerged from the study of the properties of neutrino. Chief among these findings is the fact that there has to be physics beyond the Standard Model (SM) which is a direct consequence of the neutrino oscillations. At present, the theoretical framework of neutrino mixing and masses for explaining neutrino oscillations is now firmly established. To date, the size of the mass-squared difference together with the mixing angles have been measured. However, despite the incredible precision (better than 10%) in measuring the mass-mixing parameters, the picture is not complete yet. The ordering and scale of the neutrino masses is not fully understood yet along with the value of the Dirac-phase δ_{CP}. Furthermore, flavor oscillations do not allow the probe of the nature of the neutrino fields-whether it is Dirac or Majorana.

Various programs worldwide are currently being pursued in order to provide more experimental capabilities to tackle these issues [3–11]. For instance, in order to make a precise measurement of the Dirac phase, an unprecedented amount of neutrino oscillation data will be needed in order to reduce the statistical errors. This could only be achieved with new detectors with larger mass and higher power beams.

This summary project consists of four sections. In Section II, we give a short overview of the experimental probes that led to the discovery of the neutrino oscillations. In Section III, we give the theoretical aspects of the neutrino oscillation by highlighting the definition of the survival probability. Phenomenological results are presented in Section IV. Finally, conclusions and discussion on the remaining opened problems are drawn in Section V.

II. EXPERIMENTAL PROBE OF NEUTRINO OSCILLATION PHENOMENON

Experimental evidence of neutrino oscillations can be studied from various sources: atmospheric neutrinos, nuclear-reactor neutrinos, and neutrino-antineutrino accelerator beams. The atmospheric neutrinos result from the interaction of cosmic rays and the atmosphere and mostly come from the following reactions:

$$\pi^{\pm} \longrightarrow \mu^{\pm} + \nu_{\mu}/\bar{\nu}_{\mu}, \tag{1}$$

$$\mu^{\pm} \longrightarrow e^{\pm} + \nu_{e}/\bar{\nu}_{e} + \bar{\nu}_{\mu}/\nu_{\mu}. \tag{2}$$

Production of electron-flavor antineutrino $\bar{\nu}_e$ can be accessed from nuclear reactor experiments in which $\bar{\nu}_e$ are released from the fission of the main isotopes $\left(^{235}\mathrm{U}, ^{239}\mathrm{Pu}\right)$ used in the nuclear reactors. Finally, neutrinos and anti-neutrinos can be produced from various collider experiments such as CERN, FNAL, and the Los Alamos Neutron Science Center.

Historically, one of the earliest indication of neutrino oscillations was found in solar neutrino experiments that used radiochemical techniques with the Homestake detector [12]. These experiments measured a flux of electron-flavor neutrinos ν_e, originating from the sun, that was significantly lower than the one expected by the Standard Solar Model (SSM). Because solar ν_e oscillate to different flavors, the detectors which are only sensitive to ν_e detect smaller number of events. This phenomenon has been known as the *solar neutrino problem* and has been confirmed by different neutrino experiments such as GALLEX [13, 14], Kamiokande [15–17], and Super-Kamiokande [18, 19].

The first evidence of neutrino oscillations has been established by studying the atmospheric neutrinos with water [20, 21] (Kamiokande and Super-Kamiokande) in 1998. The data exhibit a zenith angle θ dependent deficit of ν_μ which is inconsistent with calculations of neutrino atmospheric fluxes and cannot be explained by the experimental biases and uncertainties. Indeed, if neutrinos do not oscillate, the number of observed atmospheric neutrino is predicted to be uniform. In Fig.1, we see the number of observed muon-flavor neutrinos as a function of the zenith angle $\cos(\theta)$ from the Super-Kamiokande analyses. This results show that the number of *upward* going muon neutrinos generated from the outer-atmosphere is half of the number of *downward* going muon neutrino.

This observation suggested that neutrinos change flavors as they propagate from their source, (through the medium), to the detectors. Such a mechanism of flavor changes require that the neutrinos have more than one mass state which is not allowed by the SM. For this reason, the neutrino oscillation provided a direct measurement of physics beyond the SM. Hence, the search for understanding the properties of the neutrinos is considered as one of the most important directions for the search for new physics. To date, more than 40 different experiments is dedicated to the investigation of the problem of neutrino masses and mixing.

* tanjona.rabemananjara@mi.infn.it

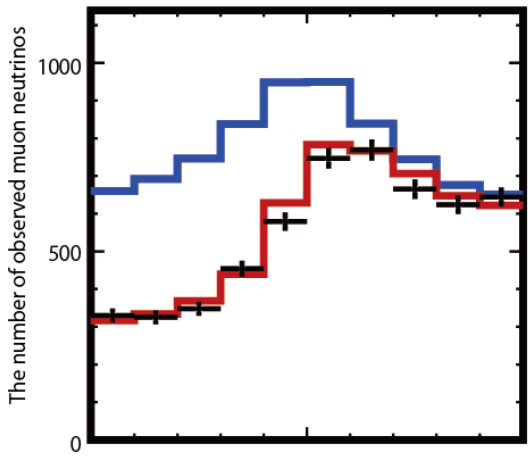

FIG. 1: Observed muon-flavor neutrino from the Super-Kamiokande experiment. The *blue* curve represents the expected number of event without neutrino oscillation, the *red* curve represents the number of events in case of neutrino oscillation, and the *black* crosses represent the observed number of events in the Super-Kamiokande detector.

III. THEORETICAL FRAMEWORK

Neutrinos interacts with other particles via weak interactions which are described by the charge current (CC) and neutral current (NC) interaction Lagrangians [22]:

$$\mathcal{L}_{CC} = -\frac{g}{2\sqrt{2}}\mathcal{J}_\rho^{CC}W^\rho + h.c, \tag{3}$$

$$\mathcal{L}_{NC} = -\frac{g}{2\cos(\theta_W)}\mathcal{J}_\rho^{NC}Z^\rho, \tag{4}$$

where g represents the $SU(2)_L$ gauge coupling constant and θ_W the weak angle. Furthermore, the charged and neutral current that are respectively denoted by $\mathcal{J}_\rho^{CC}$ and $\mathcal{J}_\rho^{NC}$ are defined as:

$$\mathcal{J}_\rho^{CC} = 2\sum_l \bar{\nu}_{lL}\gamma_\rho l_L + \cdots, \tag{5}$$

$$\mathcal{J}_\rho^{NC} = \sum_l \bar{\nu}_{lL}\gamma_\rho \nu_{lL} + \cdots, \tag{6}$$

where the charged leptonic field l can be one of the neutrino flavors (e, μ, τ) with mass m_l. Notice that in the equations above we have only written explicitly terms containing the neutrino fields.

If neutrinos have zero-masses, the left-handed neutrino field $\nu_{\alpha L}$ with flavor α can be written as a superposition of the left-handed components ν_{iL} of the neutrino field with mass m_i. In an ultra-relativistic scenario, we have:

$$\nu_{\alpha L} = U_{\alpha i}\nu_{iL} \tag{7}$$

where repeated indices are summed over. Henceforth, we use Greek letters to refer to the neutrino masses and Latin letters to refer to the flavours. The neutrino masses i runs from 1 to N where N denotes the number of massive neutrinos. In this project, we are only going to focus in the case $N = 3$.

In Eq. (7), U is a unitary matrix. This implies that, in the ultra-relativistic case, the flavor eigenstate $|\nu_\alpha\rangle$ can be written as a superposition of different mass eigenstates $|\nu_i\rangle$ in the following way:

$$|\nu_{\alpha L}\rangle = U^\star_{\alpha i}|\nu_i\rangle, \tag{8}$$

$$|\bar{\nu}_{\alpha L}\rangle = U_{\alpha i}|\bar{\nu}_i\rangle. \tag{9}$$

Assuming that we have three (03) massive neutrinos, the mixing unitary matrix U can be written as:

$$U = \begin{pmatrix} 1 & 0 & 0 \\ 0 & c_{23} & s_{23} \\ 0 & -s_{23} & c_{23} \end{pmatrix} \begin{pmatrix} c_{13} & 0 & s_{13}e^{i\delta_{13}} \\ 0 & 1 & 0 \\ -s_{13}e^{i\delta_{13}} & 0 & c_{13} \end{pmatrix} \begin{pmatrix} c_{12} & s_{12} & 0 \\ -s_{12} & c_{12} & 0 \\ 0 & 0 & 1 \end{pmatrix} \begin{pmatrix} 1 & 0 & 0 \\ 0 & e^{i\delta_{13}} & 0 \\ 0 & 0 & 1 \end{pmatrix}, \tag{10}$$

where $c_{ij} = \cos(\theta_{ij})$ and $s_{ij} = \sin(\theta_{ij})$. Here, θ_{ij} denote the mixing angles while δ denotes the Dirac-type CP-phase (often denoted here as δ_{CP}). Defining $\Delta_{ij} = m_i^2 - m_j^2$ and ordering the masses such that $\Delta_{21}^2 > 0$ and $\Delta_{21}^2 < \Delta_{31}^2$, we have the following constraints:

$$0 \leq \theta_{ij} \leq \frac{\pi}{2} \quad (i \neq j), \quad 0 \leq \delta \leq 2\pi. \tag{11}$$

III.1. Neutrino evolution equation in vacuum and in matter

The evolution equation of a generic neutrino state $|\nu(t)\rangle$ is described by a Shrödinger-like equation:

$$i\partial_t|\nu_\alpha(t)\rangle = H|\nu_\alpha(t)\rangle, \tag{12}$$

where H represents the Hamiltonian operator. Expressed in the flavor eigenstate basis $|\nu_\alpha\rangle$, the above equation translates into

$$i\partial_t\nu^{(f)}(t) = H^{(f)}\nu^{(f)}(t), \tag{13}$$

where $\nu^{(f)}(t)$ denotes the vector describing the flavor content of the neutrino state $|\nu(t)\rangle$. Elements of the Hamiltonian matrix $H^{(f)}$ are given by

$$H^{(f)}_{\alpha\beta} = \langle\nu_\alpha|H|\nu_\beta\rangle. \tag{14}$$

In the mass eigenstate basis, the vacuum Hamiltonian $H^{(m)}$ (where m indicates the mass eigenstate representation) is determined in terms of the neutrino masses

$$H^{(m)}_{vac} = \text{diag}\left(\sqrt{\vec{p}^2 + m_1^2}, \sqrt{\vec{p}^2 + m_2^2}, \sqrt{\vec{p}^2 + m_3^2}\right), \\ \approx |\vec{p}| + \frac{1}{2|\vec{p}|}\text{diag}\left(m_1^2, m_2^2, m_3^2\right). \tag{15}$$

In the first equality we assumed that the neutrino state $|\nu(t)\rangle$ can be described as a superposition of states with fixed momentum $\vec{p}$. In the last line, we used the ultra-relativistic approximation $\sqrt{\vec{p}^2+m_i^2} \sim |\vec{p}| + m_i^2/2|\vec{p}|$. The new Hamiltonian in the flavor eigenstates therefore reads

$$H^{(f)}_{\alpha\beta,vac} = U_{\alpha i} H^{(m)}_{ij,vac} U^{\dagger}_{i\beta} \tag{16}$$

In the presence of matter, we have to add the vacuum Hamiltonian an effective potential V in the evolution equation

$$i\partial_t |\nu(t)\rangle = (H_{vac} + V)\,|\nu(t)\rangle, \tag{17}$$

where in the context of SM, the effective potential is a matrix that is diagonal in the flavor basis $V^{(f)} = \mathrm{diag}\,(V_e, V_\nu, V_\tau)$.

III.2. Survival probability

Assuming that a neutrino is created a a time $t_0 = 0$ at a position $x_0 = 0$, the flavor state $|\nu(t)\rangle$ in the flavor eigenstate basis can be written as

$$\nu^{(f)}(0) = \left(\langle\nu_e|\nu(0)\rangle, \langle\nu_\mu|\nu(0)\rangle, \langle\nu_\tau|\nu(0)\rangle\right)^{\mathrm{T}}. \tag{18}$$

After some interval of time t at a given position x, its flavor has evolved according to

$$\nu^{(f)}(x) = S^{(f)}(x)\nu^{(f)}(0), \tag{19}$$

where the evolution operator S is expressed as

$$S^{(f)} = T\left[\exp\left(-\mathrm{i}\int_0^x \mathrm{d}\tilde{x}\, H^{(f)}(\tilde{x})\right)\right]. \tag{20}$$

Recall that in the ultra-relativistic limit $x \approx t$. In the above equation, T represents the time ordering operator. Therefore, the probability to detect a neutrino of flavor ν_β at a distance L from its initial position (where its initial flavor is known) is given by

$$P(\nu_\beta \longleftarrow \nu_\alpha) = |S^{(f)}_{\beta\alpha}|^2. \tag{21}$$

This implies that the survival probability $P(\nu_\alpha \longleftarrow \nu_\alpha)$ is given by the following

$$P(\nu_\alpha \longleftarrow \nu_\alpha) = 1 - P(\nu_\beta \longleftarrow \nu_\alpha). \tag{22}$$

The above expression is a consequence of the unitarity of the mixing matrix $\sum_\beta P(\nu_\beta \longleftarrow \nu_\alpha) = 1$.

III.3. Vacuum neutrino oscillations

As it was presented in the previous section, in vacuum the neutrino Hamiltonian H is constant. Hence, the evolution operator can be written as

$$S^{(f)} = U S^{(m)} U^{\dagger}. \tag{23}$$

The evolution operator in the mass eigenstate (denoted by the upper-script m) is a diagonal matrix that is function of $\phi_i = -m_i^2 x/2|\vec{p}|$,

$$S^{(m)} = \mathrm{diag}\left(\exp(i\phi_1), \exp(i\phi_2), \exp(i\phi_3)\right). \tag{24}$$

Using Eq. (21), the probability of observing a neutrino of flavor ν_α to change into a neutrino of flavor ν_β is given by the following:

$$P(\nu_\beta \longleftarrow \nu_\alpha) = \left(U_{\beta i} U^{\star}_{\alpha i} U^{\star}_{\beta j} U_{\alpha j}\right) \exp(i\phi_{ij}), \tag{25}$$

where in the ultra-relativistic limit $|\vec{p}| \sim E$ and hence $\phi_{ij} = -(\Delta_{ij} L)/(2E)$. From this result, we are now equipped with the tools needed to compute the oscillation probabilities. For the case of two-neutrino flavor mixing, we only consider one non-vanishing mixing angle θ_{ij} in the evolution operator U described by Eq. (10). The oscillation probability in Eq. (25) then leads to the following well known result

$$P(\nu_\beta \longleftarrow \nu_\alpha) = \sin^2(2\theta_{ij}) \sin^2\left(\frac{\Delta^2_{ij} L}{4E}\right). \tag{26}$$

Notice that in the above expression, α has to be different from β ($\alpha \neq \beta$), and depending on the non-vanishing mixing angle (taking into account that $i \neq j$), we end up with different flavor changes, i.e.:

$$\theta_{12} \neq 0 \Longleftrightarrow P(\nu_\mu \longleftarrow \nu_e), \tag{27}$$
$$\theta_{23} \neq 0 \Longleftrightarrow P(\nu_\tau \longleftarrow \nu_\mu), \tag{28}$$
$$\theta_{13} \neq 0 \Longleftrightarrow P(\nu_\tau \longleftarrow \nu_e). \tag{29}$$

In the three-neutrino case, by performing the same steps and using further constraint on the masses as introduced previously ($\Delta^2_{21} << |\Delta^2_{31}|$), we have for instance, for $\nu_e \longrightarrow \nu_\mu$, the following probability

$$\begin{aligned} P(\nu_\mu \longleftarrow \nu_e) =& s^2_{23} S_{23} \sin^2(2\theta_{13}) \\ &+ c^2_{23} S_{12} \sin^2(2\theta_{12}) - 8 J S_{12} S_{13}, \end{aligned} \tag{30}$$

where $S_{ij} = \sin^2\left(\Delta^2_{ij} L/(4E)\right)$ and

$$J = \frac{1}{8} \sin(2\theta_{12}) \sin(2\theta_{23}) \sin(2\theta_{13}) \cos(\theta_{13}) \sin(\delta).$$

IV. PHENOMENOLOGY OF NEUTRINO OSCILLATION PROBABILITIES

In this section, we show some phenomenological results for the case of three-neutrino probability oscillations. In lieu of doing so, we first give a very brief overview of a numerical method that allows for an exact computation of those probabilities.

IV.1. Numerical insights

From the analytical point of view, computing probabilities of flavor transition involves diagonalizing the

Hamiltonian operator. This procedure, however, can be complicated especially when one studies neutrino oscillations in matter. As is often done, careful studies of perturbative methods that lead to some approximations are used in order to compute these probabilities. As described in [23], numerical methods can bring new insights into understanding how these probabilities are computed. The resulting methods provide strategies to explore non-standard oscillations where the Hamiltonians do not have generic analytical solutions.

In this project, we follow closely the method described in Ref. [23] first introduced by Ohlsson and Snellman in Ref. [24–26]. It consists on expanding the Hamiltonian operator that enters in the expression of the evolution operator in terms of $SU(2)$ and $SU(3)$ matrices. The steps for such a calculation can be subdivided into the following steps:

- First, the Hamiltonian is expanded in terms of the Pauli matrices in the case of two-neutrino oscillation, and in terms of the Gell-Mann matrices in the case of three-neutrino flavors.
- Compute the coefficients of the expansions in terms of the components of the Hamiltonian.
- The exponent $\exp(-\mathrm{i}Ht)$ is then expanded using the Cayley-Hamilton theorem which states that any analytic function of an $n \times n$ matrix can be written as a polynomial of degree $(n-1)$ in that matrix.
- Compute the evolution operator in terms of the coefficients in the Hamiltonian series and derive the corresponding probability.

In this report, we only illustrate the case for two-neutrino oscillations. For the three-neutrino case, refer to Ref.[23]. Let us denote the two-neutrino Hamiltonian by H_2. Its expansion in terms of the Pauli matrices σ^i is given by

$$\mathrm{H}_2 = h_0 + h_i\sigma^i \qquad (i = 1, 2, 3). \tag{31}$$

The coefficients h_k are fully determined by the components of the Hamiltonian matrix and can be easily computed using the explicit expression of the Pauli matrices.

$$\begin{aligned} h_0 &= \tfrac{1}{2}\left((\mathrm{H}_2)_{11} + (\mathrm{H}_2)_{22}\right) \\ h_1 &= \mathrm{Re}\left((\mathrm{H}_2)_{12}\right) \\ h_2 &= -\mathrm{Im}\left((\mathrm{H}_2)_{12}\right) \\ h_3 &= \tfrac{1}{2}\left((\mathrm{H}_2)_{11} - (\mathrm{H}_2)_{22}\right) \end{aligned} \tag{32}$$

The evolution operator S_2 for the two-neutrino oscillations case can therefore be written as

$$\mathrm{S}_2 = \exp\left(-\mathrm{i}(h_0 + h_i\sigma^i)L\right). \tag{33}$$

The first term in the exponent does not affect the probability and therefore can be ignored. Hence, the evolution operator just becomes $\mathrm{S}_2 = \exp(-\mathrm{i}h_i\sigma^i L)$. Using Euler's formula, the above expression yields

$$\mathrm{S}_2 = \cos(|h|L) - \frac{\mathrm{i}}{|h|}\sin(|h|L)h_i\sigma^i, \tag{34}$$

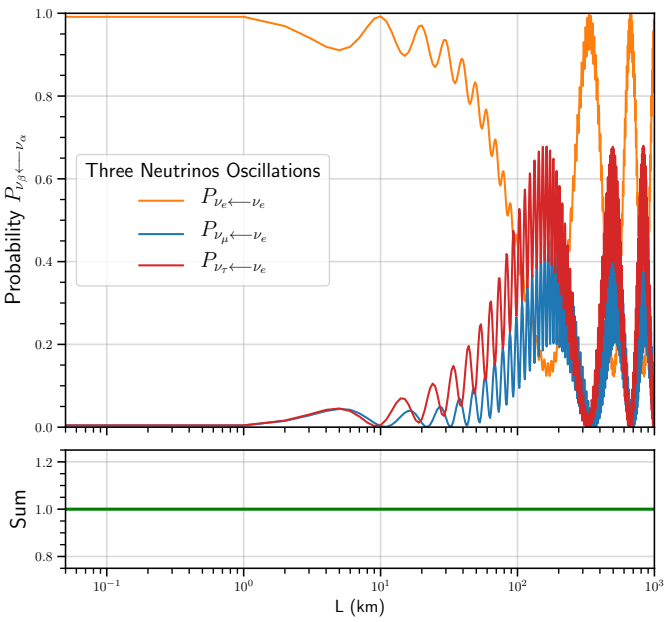

(a) Varying baseline with fixed energy $E = 10^{-2}$GeV.

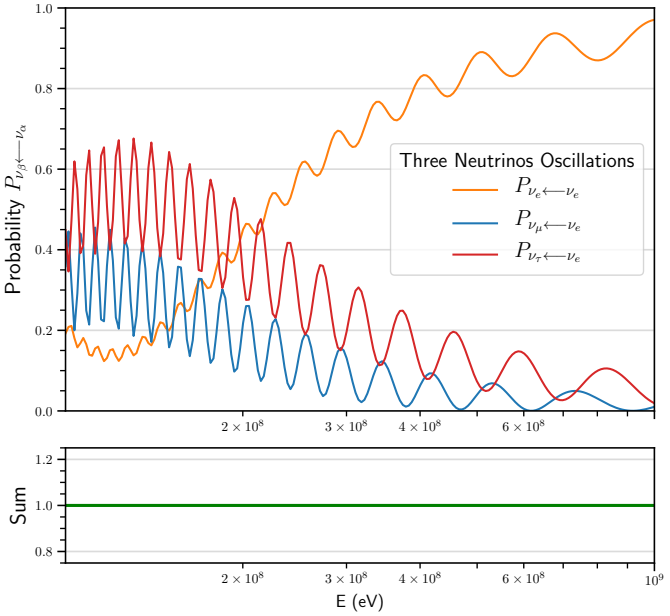

(b) Varying energy with fixed baseline $L = 2 \cdot 10^3$km.

FIG. 2: Three-neutrino oscillation probabilities in vacuum with varying (a) baseline and (b) varying energy. The top panels show the actual probabilities while the bottom panels shown the sum of the probabilities which exactly sum to one.

where $|h| = \sqrt{|h_1|^2 + |h_2|^2 + |h_3|^2}$. We can now compute the survival probability

$$P(\nu_\alpha \longleftarrow \nu_\alpha) = |\nu_\alpha^\dagger \mathrm{S}_\alpha \nu_\alpha|^2. \tag{35}$$

Considering $\nu_\alpha = (1, 0)^{\mathrm{T}}$, we can compute the terms that enter in the expression of the probability in Eq. (35)

$$\nu_\alpha^\dagger \mathrm{S}_\alpha \nu_\alpha = \cos(|h|L) - \mathrm{i}\frac{h_3}{|h|}\sin(|h|L). \tag{36}$$

Putting this expression back into Eq. (35), and with some algebras we can derive the final expression of the survival probability of a neutrino of flavor α,

$$P(\nu_\alpha \longleftarrow \nu_\alpha) = \cos^2(|h|L) + \frac{|h_3|^2}{|h|^2}\sin^2(|h|L). \quad (37)$$

Therefore, the expression of the two-neutrino oscillation probabilities–that a neutrino of flavor α is detected with a flavor β–is given by the following simple relation:

$$P(\nu_\beta \longleftarrow \nu_\alpha) = 1 - P(\nu_\alpha \longleftarrow \nu_\alpha). \quad (38)$$

Let us now show that using this approach, we re-derive the two-neutrino oscillation probability given by Eq. (26). For two-neutrino flavor oscillation, the vacuum Hamiltonian operator is defined as

$$\mathrm{H}_2^{vac} = \frac{1}{2E}\mathrm{R}_{2,\theta}\mathrm{H}_2^{(m)}\mathrm{R}_{2,\theta}^\dagger, \quad (39)$$

where $\mathrm{R}_{2,\theta}$ represents an Euler rotation with angle θ_{ij} and $\mathrm{H}_2^{(m)}$ is given by

$$\mathrm{H}_2^{(m)} = \mathrm{diag}\left(\frac{\Delta_{ij}^2}{2}, -\frac{\Delta_{ij}^2}{2}\right). \quad (40)$$

Using the coefficients h_i to compute $|h|$ and $|h_3|$, putting the explicit expression of the coefficients into Eq. (35), and doing some simplification, we arrive at the following expression

$$P(\nu_\beta \longleftarrow \nu_\alpha) = \sin^2(2\theta_{ij})\sin^2\left(\frac{\Delta_{ij}^2 L}{4E}\right), \quad (41)$$

which is exactly the same as in Eq. (35). The difference being that this approach can be easily implemented numerically to compute oscillations in matter. Going into full details of using this method to compute the three-oscillation probabilities and to study neutrino oscillations in matter (including non standard oscillations) is beyond the scope of this project and will be left aside. For complete details and computations, refer to Ref. [23]. The next section, however, will present results beyond the two-neutrino oscillations both in vacuum and in matter.

IV.2. Phenomenological results

This section is dedicated to the phenomenological study of the three-neutrino oscillations both in vacuum and in presence of matter with constant density. To compute the oscillation probabilities, the only input parameters that we vary are the energy E and the distance traveled by the neutrino L. The other parameters such as the masses and the mixing angles that enter in the expression of the Pontecorvo-Maki-Nakagawa-Sakata (PMNS) mixing matrix are extracted from the NuFit [27] code that fix the parameters to experimental data in order to find the best-fit values. These parameters are summarized in Table I.

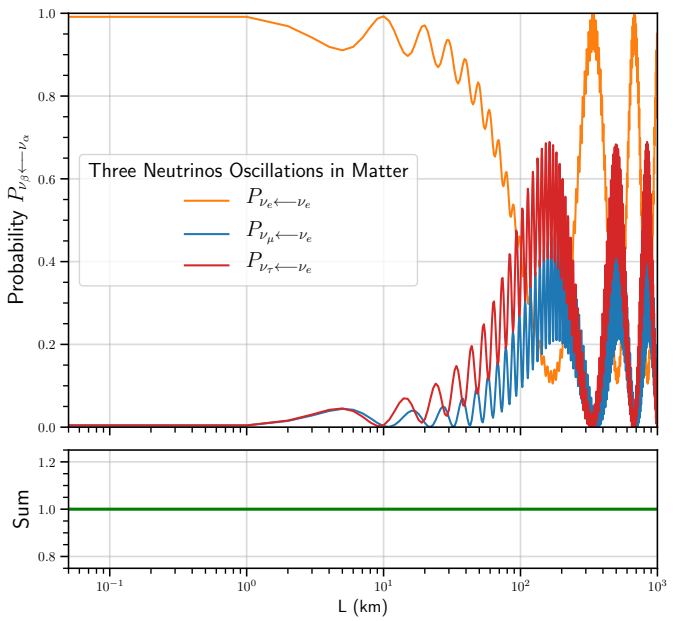

(a) Varying baseline with fixed energy $E = 10^{-2}$GeV.

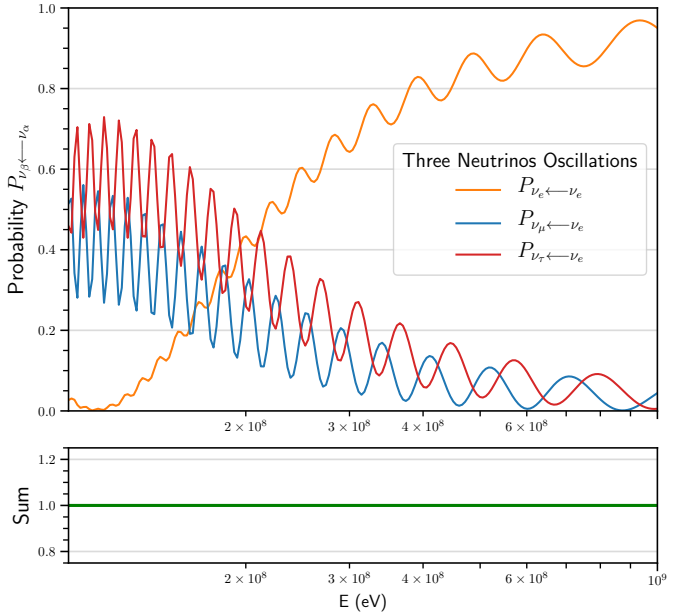

(b) Varying energy with fixed baseline $L = 2 \cdot 10^3$km.

FIG. 3: Three-neutrino oscillation probabilities in matter with varying (a) baseline and (b) varying energy. The top panels show the actual probabilities while the bottom panels shown the sum of the probabilities which exactly sum to one.

The plots shown in this project were produced using python codes [28] which in turn rely on an external python library called `NuOscProbExact` in which the numerical method presented in Ref. [23].

In Fig. 2b, we plot the three-neutrino oscillation probabilities as a function of the baseline L and energy E. In particular, we plot the probability that a neutrino with an initial flavor ν_e oscillates between flavors ν_β (with

Parameters	Numerical Values
δ_{CP}	217°
$\sin^2\theta_{12}$	0.310
$\sin^2\theta_{23}$	0.582
$\sin^2\theta_{13}$	0.022
Δ_{21}	$7.391 \cdot 10^{-5}$
Δ_{31}	$2.525 \cdot 10^{-3}$

TABLE I: Numerical values of the mass differences Δ_{ij} and mixing angles θ_{ij} extracted from a global fit to oscillation data [27].

$\beta = e, \mu, \tau$). We can clearly see in the bottom panels that the sum of all probabilities exactly gives one. For small values of L, we see that the probability that the electron-neutrino does not oscillate is high. As the neutrino traverses more distances, this probability fluctuates, and in some regions smaller than the probability of the neutrino to have a flavor ν_μ or ν_τ. In the case of probabilities as a function of energy with fixed baseline, we see that instead as the energy increases, the probability that the neutrino keeps the same flavor is higher. In Fig. 3b, we show the three-neutrino oscillation probabilities for a neutrino that propagates in a matter with constant density $\rho = 3\,g/cm^3$. As we can see, the general behavior of the curves look similar to the propagation in vacuum. In order to see the differences, we show in Fig. 4b comparisons between propagation in vacuum and in a matter for $P(\nu_\mu \longleftarrow \nu_e)$. The bottom panels show the relative difference $(P_{vac} - P_{mat})/P_{mat}$. We can notice that for small distances (even at small energies), the matter has little effect on the oscillation probability. It is worth mentioning that the propagation in a matter with constant density is the simplest case and does not fully characterize realistic scenarios. A more realistic scenario, for instance, is the study of a neutrino traversing layers of matter, each with constant, but different density as in Ref. [29–31]. Another well studied phenomena is neutrino oscillation with non-standard interactions. This takes into account the fact that the medium in which the neutrino is propagating in can affect its dynamics Ref. [32–36].

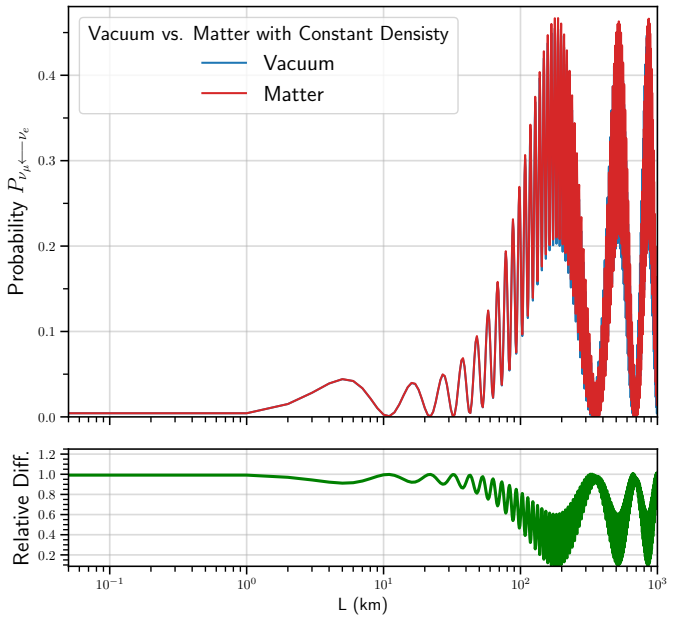

(a) Varying baseline with fixed energy $E = 10^{-2}$GeV.

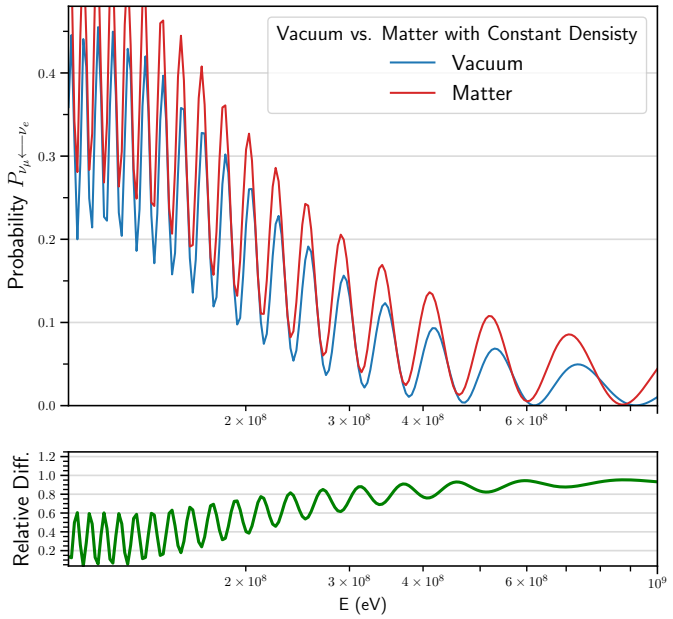

(b) Varying energy with fixed baseline $L = 2 \cdot 10^3$km.

FIG. 4: Three-neutrino oscillation probabilities in matter with varying (a) baseline and (b) varying energy. The top panels show the probability $(P_{vac} - P_{mat})/P_{mat}$ both in vacuum and in presence of matter. The bottom panels plot the relative differences.

V. CONCLUSION & PERSPECTIVES

The fact that neutrinos have masses, which is a direct consequence of the neutrino oscillation, is a concrete evidence of a physics beyond the current standard model (SM). This project attempted to give a brief overview and introduction into the field of neutrino oscillation by focusing mainly on the computation of the oscillation probabilities.

Section II described the experimental probes of the neutrino oscillation phenomena that led to its discovery. In Section III, we presented a condensed review of the theoretical framework behind the physics of neutrino oscillations. In particular, we focused on the analytical computation of the oscillation probability (and survival probability). Then, in Section IV we presented some phenomenological results concerning the neutrino oscillation probabilities both as a function of the energy and the baseline. We specifically studied the case for the three-flavor oscillation. This has been achieved with the means of a numerical approach that overcome the problems of diagonalizing the Hamiltonian in the analytical approach.

Albeit the field of neutrino oscillation physics has

achieved quite some progresses in the last couple of decades, there are still many open problems that await to be unveiled. As briefly alluded in the previous sections, some of the relevant issues concern the determination of neutrino mass hierarchy and the precise determination of the mixing angle θ_{23}. The issue of mass hierarchy might be resolved by the study of atmospheric neutrino oscillations as they are sensitive to the mass ordering through matter effects for neutrino traversing the earth's atmosphere. There are, on the other hand, issues that require high-precision experiments of not so immediate in future, such as the precise measurement of the Dirac-phase δ_{CP} and the probes of the CP violation in the leptonic sector [37]. One of the prominent future experiments is the T2HK (Hyper-Kamiokande) that will be the successor of T2K [38]. It is thus clear that high precision detectors and reactors will play a crucial role in addressing these issues.

[1] B. Pontecorvo. Mesonium and anti-mesonium. *Sov. Phys. JETP*, 6:429, 1957.

[2] B. Pontecorvo. Inverse beta processes and nonconservation of lepton charge. *Sov. Phys. JETP*, 7:172–173, 1958. [Zh. Eksp. Teor. Fiz.34,247(1957)].

[3] R. Acciarri et al. Long-Baseline Neutrino Facility (LBNF) and Deep Underground Neutrino Experiment (DUNE). 2015.

[4] M. Antonello et al. A Proposal for a Three Detector Short-Baseline Neutrino Oscillation Program in the Fermilab Booster Neutrino Beam. 2015.

[5] Fengpeng An et al. Neutrino Physics with JUNO. *J. Phys.*, G43(3):030401, 2016. doi:10.1088/0954-3899/43/3/030401.

[6] Zelimir Djurcic et al. JUNO Conceptual Design Report. 2015.

[7] P. Adamson et al. First measurement of electron neutrino appearance in NOvA. *Phys. Rev. Lett.*, 116(15):151806, 2016. doi:10.1103/PhysRevLett.116.151806.

[8] Soo-Bong Kim. New results from RENO and prospects with RENO-50. *Nucl. Part. Phys. Proc.*, 265-266:93–98, 2015. doi:10.1016/j.nuclphysbps.2015.06.024.

[9] P. Adamson et al. First measurement of muon-neutrino disappearance in NOvA. *Phys. Rev.*, D93(5):051104, 2016. doi:10.1103/PhysRevD.93.051104.

[10] K. Abe et al. Measurements of neutrino oscillation in appearance and disappearance channels by the T2K experiment with 6.6×10^{20} protons on target. *Phys. Rev.*, D91(7):072010, 2015. doi:10.1103/PhysRevD.91.072010.

[11] C. Adams et al. The Long-Baseline Neutrino Experiment: Exploring Fundamental Symmetries of the Universe. In *Snowmass 2013: Workshop on Energy Frontier Seattle, USA, June 30-July 3, 2013*, 2013. URL http://lss.fnal.gov/archive/2014/pub/fermilab-pub-14-022.pdf.

[12] B. T. Cleveland, Timothy Daily, Raymond Davis, Jr., James R. Distel, Kenneth Lande, C. K. Lee, Paul S. Wildenhain, and Jack Ullman. Measurement of the solar electron neutrino flux with the Homestake chlorine detector. *Astrophys. J.*, 496:505–526, 1998. doi:10.1086/305343.

[13] W. Hampel et al. GALLEX solar neutrino observations: Results for GALLEX III. *Phys. Lett.*, B388:384–396, 1996. doi:10.1016/S0370-2693(96)01121-5.

[14] P. Anselmann et al. GALLEX solar neutrino observations: The Results from GALLEX-I and early results from GALLEX-II. *Phys. Lett.*, B314:445–458, 1993. doi:10.1016/0370-2693(93)91264-N.

[15] K. S. Hirata et al. Observation in the Kamiokande-II Detector of the Neutrino Burst from Supernova SN 1987a. *Phys. Rev.*, D38:448–458, 1988. doi:10.1103/PhysRevD.38.448.

[16] K. S. Hirata et al. Real time, directional measurement of B-8 solar neutrinos in the Kamiokande-II detector. *Phys. Rev.*, D44:2241, 1991. doi:10.1103/PhysRevD.44.2241, 10.1103/PhysRevD.45.2170. [Erratum: Phys. Rev.D45,2170(1992)].

[17] Y. Fukuda et al. Solar neutrino data covering solar cycle 22. *Phys. Rev. Lett.*, 77:1683–1686, 1996. doi:10.1103/PhysRevLett.77.1683.

[18] Y. Fukuda et al. Measurements of the solar neutrino flux from Super-Kamiokande's first 300 days. *Phys. Rev. Lett.*, 81:1158–1162, 1998. doi:10.1103/PhysRevLett.81.1158, 10.1103/PhysRevLett.81.4279. [Erratum: Phys. Rev. Lett.81,4279(1998)].

[19] C. Giunti, C. W. Kim, U. W. Lee, and Vadim A. Naumov. Implications of Super-Kamiokande atmospheric low-energy data for solar neutrino oscillations. 1999.

[20] Y. Fukuda et al. Evidence for oscillation of atmospheric neutrinos. *Phys. Rev. Lett.*, 81:1562–1567, 1998. doi:10.1103/PhysRevLett.81.1562.

[21] Y. Ashie et al. Evidence for an oscillatory signature in atmospheric neutrino oscillation. *Phys. Rev. Lett.*, 93:101801, 2004. doi:10.1103/PhysRevLett.93.101801.

[22] Samoil M. Bilenky, C. Giunti, and W. Grimus. Phenomenology of neutrino oscillations. *Prog. Part. Nucl. Phys.*, 43:1–86, 1999. doi:10.1016/S0146-6410(99)00092-7.

[23] Mauricio Bustamante. NuOscProbExact: a general-purpose code to compute exact two-flavor and three-flavor neutrino oscillation probabilities. 2019.

[24] Tommy Ohlsson and Hakan Snellman. Three flavor neutrino oscillations in matter. *J. Math. Phys.*, 41:2768–2788, 2000. doi:10.1063/1.533270. [Erratum: J.Math.Phys. 42, 2345 (2001)].

[25] Tommy Ohlsson and Hakan Snellman. Neutrino oscillations with three flavors in matter: Applications to neutrinos traversing the Earth. *Phys. Lett. B*, 474:153–162, 2000. doi:10.1016/S0370-2693(00)00008-3. [Erratum: Phys.Lett.B 480, 419–419 (2000)].

[26] Tommy Ohlsson and Hakan Snellman. Neutrino oscillations with three flavors in matter of varying density. *Eur. Phys. J. C*, 20:507–515, 2001. doi:10.1007/s100520100687.

[27] Ivan Esteban, M. C. Gonzalez-Garcia, Alvaro Hernandez-Cabezudo, Michele Maltoni, and Thomas Schwetz. Global analysis of three-flavour neutrino oscillations: synergies and tensions in the determination of θ_{23}, δ_{CP}, and the mass ordering. *JHEP*, 01:106, 2019. doi:10.1007/JHEP01(2019)106.

[28] Tanjona R. Neutrino Oscillation Probabilities, Septem-

ber 2020. URL https://github.com/Radonirinaunimi/NeutrinoProject.

[29] M. V. Chizhov and S. T. Petcov. New conditions for a total neutrino conversion in a medium. *Phys. Rev. Lett.*, 83:1096–1099, 1999. doi:10.1103/PhysRevLett.83.1096.

[30] M. V. Chizhov and S. T. Petcov. Enhancing mechanisms of neutrino transitions in a medium of nonperiodic constant density layers and in the earth. *Phys. Rev.*, D63: 073003, 2001. doi:10.1103/PhysRevD.63.073003.

[31] Kara M. Merfeld and David C. Latimer. Parametric enhancement of flavor oscillation in a three-neutrino framework. *Phys. Rev.*, C90(6):065502, 2014. doi: 10.1103/PhysRevC.90.065502.

[32] Bjorn Jacobsson, Tommy Ohlsson, Hakan Snellman, and Walter Winter. Effects of random matter density fluctuations on the neutrino oscillation transition probabilities in the Earth. *Phys. Lett.*, B532:259–266, 2002. doi: 10.1016/S0370-2693(02)01580-0.

[33] Tommy Ohlsson and Walter Winter. The Role of matter density uncertainties in the analysis of future neutrino factory experiments. *Phys. Rev.*, D68:073007, 2003. doi: 10.1103/PhysRevD.68.073007.

[34] C. A. Argüelles, M. Bustamante, and A. M. Gago. Searching for cavities of various densities in the Earth's crust with a low-energy $\bar{\nu}_e$ β-beam. *Mod. Phys. Lett.*, A30 (29):1550146, 2015. doi:10.1142/S0217732315501461.

[35] Byron Roe. Matter density versus distance for the neutrino beam from Fermilab to Lead, South Dakota, and comparison of oscillations with variable and constant density. *Phys. Rev.*, D95(11):113004, 2017. doi: 10.1103/PhysRevD.95.113004.

[36] Kevin J. Kelly and Stephen J. Parke. Matter Density Profile Shape Effects at DUNE. *Phys. Rev.*, D98(1): 015025, 2018. doi:10.1103/PhysRevD.98.015025.

[37] Francesco Capozzi, Eleonora Di Valentino, Eligio Lisi, Antonio Marrone, Alessandro Melchiorri, and Antonio Palazzo. Global constraints on absolute neutrino masses and their ordering. *Phys. Rev. D*, 95(9):096014, 2017. doi: 10.1103/PhysRevD.95.096014. [Addendum: Phys.Rev.D 101, 116013 (2020)].

[38] G. Bellini, L. Ludhova, G. Ranucci, and F. L. Villante. Neutrino oscillations. *Adv. High Energy Phys.*, 2014: 191960, 2014. doi:10.1155/2014/191960.